Hindawi
Advances in Mathematical Physics
Volume 2020, Article ID 5782457, 8 pages
https://doi.org/10.1155/2020/5782457

Research Article

Deviation Effect of Coaxiality on the Rock Brazilian Split

Zenghui Zhao,[1,2] **Mingzhong Zhang**,[1,2] **Qing Ma**,[1,2] **and Baosen Chen**[1,2]

[1]*State Key Laboratory of Mining Disaster Prevention and Control Co-founded by Shandong Province and the Ministry of Science and Technology, Qingdao 266590, China*
[2]*College of Mining and Safety Engineering, Shandong University of Science and Technology, Qingdao 266590, China*

Correspondence should be addressed to Zenghui Zhao; tgzyzzh@163.com

Received 5 September 2019; Revised 10 November 2019; Accepted 30 December 2019; Published 1 February 2020

Academic Editor: Nicola L. Rizzi

Tension failure is one of the main forms of instability in geotechnical engineering. Aiming at the calculation error caused by the loading direction deviation of the Brazilian disc splitting method, a mechanical model of a disc under chord loading was constructed firstly. Based on the theory of complex variable function, the analytic solutions of stresses in a circular disc were deduced, and the calculation error of the tensile strength under chord loading was characterized by defining the error impact rate. And the stress distribution of a disc and the law of rock fracture under chord loading were detailed analyzed through numerical calculation. Through numerical calculation, the stress distribution of the disc and rock failure law under chordwise loading are discussed in detail. The results show that the stress concentration near the loading point is stronger under the chordwise loading comparing with the radial loading, which makes the disc more vulnerable to produce compression failure near the loading point. The disc exhibits a maximum tensile stress and a minimum compressive stress at the intersection of the loaded string and the horizontal diameter, so that tensile rupture damage is likely to occur here. With the increase of deviation angle, the tensile strength measured by the Brazilian splitting test decreases gradually, and the influence rate of error increases significantly. The proposed analytical solution under chord loading provides theoretical guiding significance for nonradial splitting failure of a disc.

1. Introduction

The tensile strength of rock is far lower than the compressive strength, so tension failure is one of the main forms of instability in many geotechnical engineering [1–3]. Thus, in the design and construction of underground engineering, the rock tensile strength is a very important mechanical index, which often controls the strength and stability of rock structures [4–6]. Accurate access to this key parameter is of great significance for various types of geotechnical disaster prevention and control.

For a long time, in order to obtain the tensile strength, engineers and researchers have proposed many experimental methods, such as a direct tension method, splitting method, bending experimental method, and point-load fracturing method [7, 8], and carried out a lot of analysis and discussion on the advantages and disadvantages of these methods [9, 10]. Due to the difficulties of sample processing, loading process (clamping, alignment, and how to eliminate bending moment, torque, etc.) in direct tension tests, the Brazilian splitting indirect test method is widely used in geotechnical engineering at home and abroad [11, 12]. This method was recommended by ISRM in 1978 as a preferred method for determining rock tensile strength [13]. The so-called Brazilian splitting is a test in which the diameter of a cylindrical (also known as a Brazilian disc) specimen is subjected to two opposite point loads in the radial direction, so that the specimen is destroyed along its diameter. From the current research results, tensile strength measured by a splitting test is still quite discrete and is affected by many factors, such as the thickness of disc specimen, the contact mode of the load, and the size of the spacer. For example, aiming at the size effect [14–17] caused by the thickness to diameter ratio, the result shows that the tensile stress on the axle wire of the disc is not a constant but a high-end, low-middle distribution, with an obvious spatial effect. At the same time, the compression failure near the loading point of the disc violates the hypothesis of the initiation of the crack from

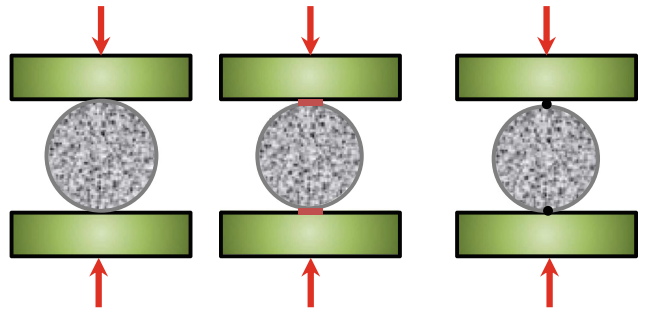

Figure 1: Diagram of loading mode for diametral splitting.

the center of the disc due to the strong stress concentration. In order to improve the effect of end surface, researchers have proposed arc loading and platform loading methods [18, 19], which revised the theoretical calculation formula for the radial loading. The results show that the distribution of face load and friction effect have an important influence on the disc rupture characteristics [20–24]. In addition, the influence of the spacer method cannot be neglected [25]. For hard rock, spacer types can be divided into a hard spacer and a soft spacer. The tensile strength measured by a soft spacer method is obviously larger than that by a hard spacer method, because the direct bearing area of specimen is increased. But the experimental dispersion of a hard spacer is smaller.

From the existing results, although the Brazilian splitting test of diameter compression of a disc is recommended by the code [13] for testing rock tensile strength, there are still many uncertainties and drawbacks. Researchers have done a lot of research on the discreteness of splitting strength caused by a size effect, effect of end surface loading, and spacer effect by means of experimental test, theoretical calculation, and numerical simulation. By weakening the influence of these effects, the testing accuracy of tensile strength can be further improved. Relevant experiments show that the size effect caused by the diameter and thickness of the disc is not remarkable [26], but heterogeneity and anisotropy of rock materials are uncontrollable factors. In fact, the coaxiality of the disc and the spacer is also an important factor. If there is a deviation between the loading line of action and the radial line of the disc, it will have an important impact on the stress distribution of the disc, which will inevitably lead to the change of the crack starting point position. However, the research on this problem is rare. To this end, this paper will analyze the influence of the coaxiality deviation on the splitting effect, in order to quantitatively give the tensile strength error caused by such deviation, and provide the theoretical guidance for the splitting test loading.

2. Stress Solution under Chord Loading of Brazilian Splitting

2.1. Chord Splitting Model of a Brazilian Disc. At present, there are three main loading methods for diametral loading

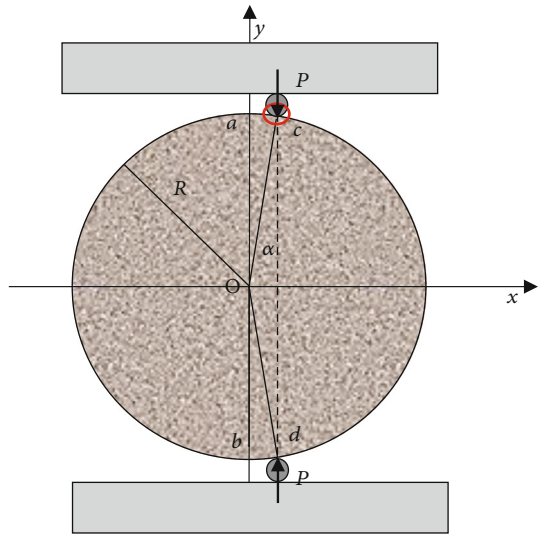

Figure 2: The compressed disc in the chord direction.

Brazilian splitting experiments, as shown in Figure 1. Whether the spacer is added to the loading point or which spacer is added is not mandatory in the specification. Figure 1(a) shows the direct loading, that is, the sample is in direct contact with the loading platen. This method is the easiest. Figure 1(b) shows the use of spacers. This loading method increases the contact area between the rock sample and the platen. However, due to the low strength, the spacer will be crushed and adhered to the rock sample after the experiment. Figure 1(c) is the wire loading. The wire must be glued to the sample beforehand during the experiment. This is the most difficult of the three methods.

In these loading modes, there is difficulty in the alignment of the sample during loading, that is, it is difficult to ensure that the loading line is along the radial direction of the disc, but along the chordwise direction, which will cause deviation of the experimental results. As shown in Figure 2, it is assumed that the disc of radius R does not achieve the diameter loading along the ab diameter but bears the load P along the chordwise cd due to the slight deviation. The force on the disc at point C is shown in Figure 3. The radial force and friction force can be combined into a force, which is consistent with P, since P is the fracture load, for simplicity and

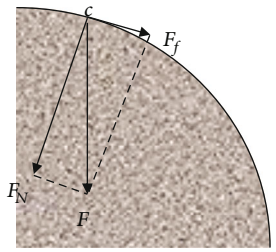

Figure 3: Detail view of the disc force.

clarity, in the subsequent part of the article so that P is used to derive the formula. Figure 4 shows the mechanical model of the compression disk, and β represents the deviation degree of loading.

According to the complex variable function theory, the stress of the disc satisfies the following equation.

$$\begin{aligned} \sigma_y + \sigma_x &= 4\,\mathrm{Re}\left[\varphi'(z)\right], \\ \sigma_y - \sigma_x + 2i\tau_{xy} &== 2\left[\bar{z}\varphi''(z) + \psi'(z)\right], \end{aligned} \tag{1}$$

where $\varphi(z)$ and $\psi(z)$ are called Kolosov-Muskhelishvili function, i.e., K-M analytic function.

2.2. Determination of the K-M Function of the Circular Domain Problem. The complex variables in the disc region D satisfy $|z| < R$ and $|z| = R$ on the boundary L. The complex variable on the boundary is changed to σ. Then, the stress boundary condition is

$$f(\sigma) = i\int_A^B \left(\bar{f}_x + i\bar{f}_y\right) ds, \tag{2}$$

where $\sigma = \mathrm{Re}^{i\theta}$, $0 \le \theta \le 2\pi$, $f(\sigma)$ represents the principal vector of surface force between base point A and any point B on boundary S, and $\bar{f}_x$ and $\bar{f}_y$ are the surface forces along the x, y direction on the boundary S.

According to the complex variable function theory, two analytic functions $\varphi(z)$ and $\psi(z)$ in D should satisfy on the boundary [27]

$$\varphi(\sigma) + \sigma\overline{\varphi'(\sigma)} + \overline{\psi(\sigma)} = f(\sigma). \tag{3}$$

Conjugated on both sides of the above equation,

$$\overline{\varphi(\sigma)} + \bar{\sigma}\varphi'(\sigma) + \psi(\sigma) = \overline{f(\sigma)}. \tag{4}$$

Equations (3) and (4) are simultaneously divided by $2\pi i$ $(\sigma - z)$ and integrated over the boundary L.

$$\begin{aligned} &\frac{1}{2\pi i}\oint_L \frac{\varphi(\sigma)}{\sigma - z}d\sigma + \frac{1}{2\pi i}\oint_L \frac{\sigma\overline{\varphi'(\sigma)}}{\sigma - z}d\sigma + \frac{1}{2\pi i}\oint_L \frac{\overline{\psi(\sigma)}}{\sigma - z}d\sigma \\ &\quad = \frac{1}{2\pi i}\oint_L \frac{f(\sigma)}{\sigma - z}d\sigma, \end{aligned} \tag{5}$$

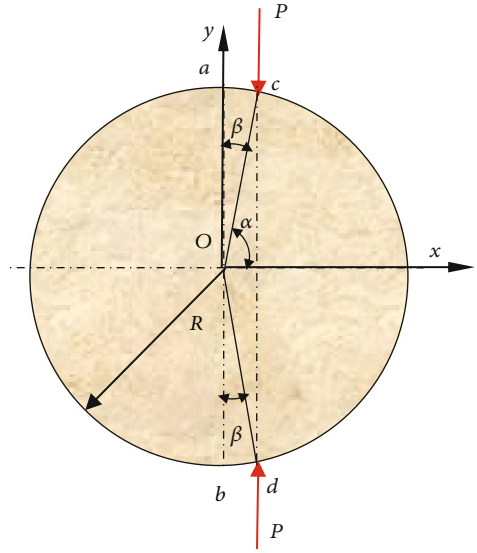

Figure 4: Mechanical model of compressed disk.

$$\begin{aligned} &\frac{1}{2\pi i}\oint_L \frac{\overline{\varphi(\sigma)}}{\sigma - z}d\sigma + \frac{1}{2\pi i}\oint_L \frac{\bar{\sigma}\varphi'(\sigma)}{\sigma - z}d\sigma + \frac{1}{2\pi i}\oint_L \frac{\psi(\sigma)}{\sigma - z}d\sigma \\ &\quad = \frac{1}{2\pi i}\oint_L \frac{\overline{f(\sigma)}}{\sigma - z}d\sigma. \end{aligned} \tag{6}$$

The two analytic functions in D can be written as the following power series.

$$\begin{aligned} \varphi(z) &= \sum_{n=1}^{\infty} a_n z_n, \\ \psi(z) &= \sum_{n=1}^{\infty} b_n z_n, \end{aligned} \tag{7}$$

where a_1 and b_1 are real constants, that is, $a_1 = \bar{a}_1$, $b_1 = \bar{b}_1$.

Substituting Equation (7) into Equations (5) and (6) and using well-known properties of Cauchy-type integral, this leads to the as follows expression of determining two analytic functions.

$$\varphi(z) = \frac{1}{2\pi i}\oint_L \frac{f(\sigma)}{\sigma - z}d\sigma - \frac{z}{4\pi i}\oint_L \frac{f(\sigma)}{\sigma^2}d\sigma, \tag{8}$$

$$\psi(z) = \frac{1}{2\pi i}\oint_L \frac{\overline{f(\sigma)}}{\sigma - z}d\sigma - R^2\frac{\varphi'(z)}{z} + \frac{R^2}{4\pi i z}\oint_L \frac{f(\sigma)}{\sigma^2}d\sigma. \tag{9}$$

2.3. Stress Solution of Chord Splitting of a Disc. The boundary condition of the disc chord loading problem of Figure 4 is

$$f(\sigma) = \begin{cases} 0, & 0 \le \theta < \alpha,\ 2\pi - \alpha \le \theta < 2\pi, \\ \dfrac{P}{t}, & \alpha \le \theta < 2\pi - \alpha, \end{cases} \tag{10}$$

where P is the fracture load and t is the thickness of the disk. $f(\sigma)$ is a function of force per unit thickness.

The position of point c at the action of P is denoted as $\sigma_1 = \mathrm{Re}^{i\alpha}$, and the position of point d is denoted as $\sigma_2 = \mathrm{Re}^{i(2\pi-\alpha)} = \mathrm{Re}^{-i\alpha}$, which can be obtained by using Equation (10).

$$\frac{1}{2\pi i}\oint_L \frac{f(\sigma)}{\sigma - z}d\sigma = \frac{1}{2\pi i}\int_{\sigma_1}^{\sigma_2}\frac{P}{\sigma - z}d\sigma = \frac{P}{2\pi i}\ln\frac{\sigma_2 - z}{\sigma_1 - z}, \tag{11}$$

$$\frac{1}{2\pi i}\oint_L \frac{\overline{f(\sigma)}}{\sigma - z}d\sigma = \frac{1}{2\pi i}\int_{\sigma_1}^{\sigma_2}\frac{P}{\sigma - z}d\sigma = \frac{P}{2\pi i}\ln\frac{\sigma_2 - z}{\sigma_1 - z}, \tag{12}$$

$$\frac{1}{4\pi i}\oint_L \frac{f(\sigma)}{\sigma^2}d\sigma = \frac{1}{4\pi i}\int_{\sigma_1}^{\sigma_2}\frac{P}{\sigma^2}d\sigma = \frac{P}{4\pi i}\left(\frac{1}{\sigma_1} - \frac{1}{\sigma_2}\right) = \frac{1}{4\pi i}\frac{\bar{\sigma}_1 - \bar{\sigma}_2}{R^2}. \tag{13}$$

Substituting Equations (11)~(13) into Equations (8) and (9), respectively, can obtain expressions of two analytic functions as follows:

$$\varphi(z) = -\frac{p}{2\pi i}\left[\ln(\sigma_1 - z) - \ln(\sigma_2 - z) - \frac{(\bar{\sigma}_1 - \bar{\sigma}_2)z}{2R^2}\right], \tag{14}$$

$$\psi(z) = \frac{p}{2\pi i}\left[\ln(\sigma_2 - z) - \ln(\sigma_1 - z) + \frac{\bar{\sigma}_2}{\sigma_2 - z} - \frac{\bar{\sigma}_1}{\sigma_1 - z}\right], \tag{15}$$

where $\sigma_1 - \sigma_2 = 2iR\sin\alpha$, $\bar{\sigma}_1 - \bar{\sigma}_2 = -2iR\sin\alpha$. Substituting Equations (14) and (15) into Equation (1) and considering that $z = x + iy$, $\alpha + \beta = 90^\circ$, the stress solution for the chordwise loading is obtained as follows:

$$\begin{aligned}\sigma_x &= -\frac{2P}{\pi t}\Phi_1(\beta, x, y),\\ \sigma_y &= -\frac{2P}{\pi t}\Phi_2(\beta, x, y),\\ \tau_{xy} &= -\frac{2P}{\pi t}\Phi_3(\beta, x, y),\end{aligned} \tag{16}$$

where

$$\begin{aligned}\Phi_1(\beta, x, y) &= \frac{(R\sin\beta - x)^2(R\cos\beta - y)}{\left[(R\sin\beta - x)^2 + (R\cos\beta - y)^2\right]^2}\\ &\quad + \frac{(R\sin\beta - x)^2(R\cos\beta + y)}{\left[(R\sin\beta - x)^2 + (R\cos\beta + y)^2\right]^2} - \frac{\cos\beta}{2R},\\ \Phi_2(\alpha, x, y) &= \frac{(R\cos\beta - y)^3}{\left[(R\sin\beta - x)^2 + (R\cos\beta - y)^2\right]^2}\\ &\quad + \frac{(R\cos\beta + y)^3}{\left[(R\sin\beta - x)^2 + (R\cos\beta - y)^2\right]^2} - \frac{\cos\beta}{2R},\\ \Phi_3(\alpha, x, y) &= \frac{(R\cos\beta - y)^2(R\sin\beta - x)}{\left[(R\sin\beta - x)^2 + (R\cos\beta - y)^2\right]^2}\\ &\quad + \frac{(R\cos\beta + y)^2(R\sin\beta - x)}{\left[(R\sin\beta - x)^2 + (R\cos\beta + y)^2\right]^2}.\end{aligned} \tag{17}$$

3. Error Impact Rate of Chordwise Loading

In Equation (16), when $\beta = 0^\circ$, it is the diameter loading, thus

$$\Phi_1(0^\circ, x, y) = \frac{x^2(R - y)}{\left[x^2 + (R - y)^2\right]^2} + \frac{x^2(R + y)}{\left[x^2 + (R + y)^2\right]^2} - \frac{1}{2R}. \tag{18}$$

The above function takes the extremum at the circle center and is denoted as

$$\sigma_t = \sigma_{x\,\max} = -\frac{2P}{\pi t}\Phi_1(0^\circ, 0, 0) = -\frac{P}{\pi R t}. \tag{19}$$

This is the most widely used formula for determining rock tensile strength at present. The error impact rate of the coaxiality of the loading point and the axis of a circular disc on the tensile strength is discussed below. Here, the error impact rate is defined as follows:

$$\eta = \frac{\sigma_{x\,\max}(\beta) - \sigma_{x\,\max}(0^\circ)}{\sigma_{x\,\max}(0^\circ)} \times 100\%. \tag{20}$$

Substituting Equation (16) into (20),

$$\eta = \frac{\Phi_{1\,\max}(\beta) - \Phi_{1\,\max}(0^\circ)}{\Phi_{1\,\max}(0^\circ)} \times 100\%. \tag{21}$$

4. Result Analysis and Discussion

4.1. Stress Distribution of a Disc with Deviation of Coaxiality. Figure 5 shows horizontal stress cloud at different deviation angles, Figure 5(a) is a cloud of $\beta = 0^\circ$ versus diameter loading, and the loading diameter is the axis of symmetry in the disc, forming a flower-shaped pull with a wide central portion and a narrow end. As the deviation angle β increases, the tensile stress region moves to the right and gradually contracts. The stress cloud is in the shape of a flower, which is divided by loaded chord direction into two parts: the left side is sparse, the right side is dense, and the right side has a large tensile stress area. The greater the loading deviation, the more severe the stress concentration at the loading point, and the greater the probability that the disc will first be damaged at the loading points at both ends.

Figure 6 further shows the horizontal stress distribution along the action line of the loading force under different deviation angles. In order to facilitate the drawing without losing the general law, this figure takes 80% of the length of the loaded string. It can be seen from the figure that the horizontal stress in the middle of the loaded chord is almost uniformly distributed tensile stress. As the deviation angle increases, the tensile stress on the loading chord decreases gradually, from 6.36 MPa at 0° to 6.27 MPa at 10°. Near the loading point, the tensile stress area decreases gradually and becomes the compressive stress area.

Figure 7 shows the stress distribution along the horizontal diameter at different deviation angles. Figure 7(a) shows the variation of tensile stress distribution. The curve

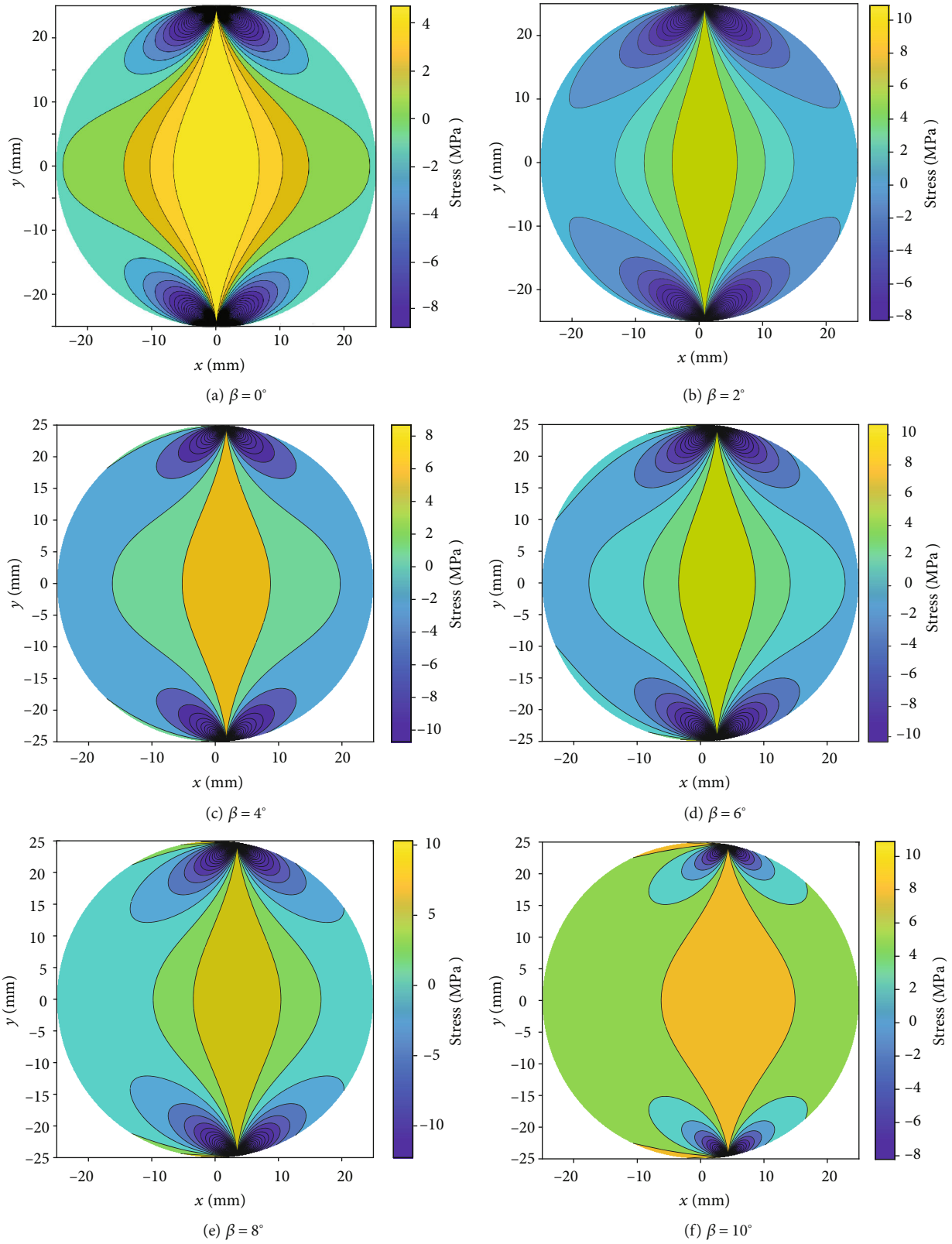

Figure 5: Horizontal stress cloud diagram at different deviation angles β.

is mountain-like. When $\beta = 0°$, the tensile stress reaches the maximum at the midpoint. As the deviation angle increases, the peak gradually shifts to the right. The maximum value of tensile stress is obtained at the intersection of loading chord and diameter. Figure 7(b) shows the distribution of compressive stress along the horizontal line.

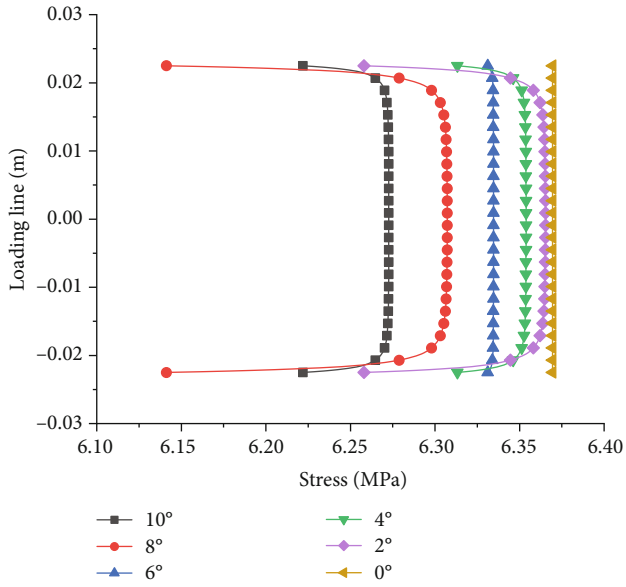

Figure 6: Distribution of tensile stress along the loading line at different deviation angles.

The curve is valley-like. When $\beta = 0°$, the compressive stress reaches the minimum at the midpoint. As the deviation angle increases, the trough gradually shifts to the right, and the compressive stress which is the maximum value is obtained at the intersection of the loaded string and the diameter.

From the above analysis, the horizontal stress distribution under the bias loading is similar to the diametrical loading, and the stress contour distribution gradually shifts to the right as the deviation angle increases, forming a sparse stress distribution on the right side of the dense side. The stress concentration of the horizontal and vertical stresses at the loading point increases with the increase of the deviation angle. This increases the possibility of compression failure of the disc near the loading point. The tensile stress increases gradually along the line of action of the loading force, and the maximum tensile stress region appears in the vicinity of the midpoint. The Brazilian disc test under the bias loading also has a splitting phenomenon, and the cracking point is at the midpoint of the loading string, that is, the intersection of the loading force line and the horizontal diameter. However, the tensile stress decreases with the increase of the deviation angle, which will cause the tensile strength measured by the Brazilian disc split test to be lower than the tensile strength of the radial load.

4.2. Influence of Coaxiality Deviation on Splitting Strength and Formula Correction. Figure 8 shows the evolution law of the influence of the chord loading with the deviation angle by using Equation (21). As the deviation angle increases, the error impact rate increases gradually, and the rate of change becomes larger and larger. When $\beta = 2°$, the error impact rate is only 0.06%, and when $\beta = 10°$, the error impact rate is 1.52%. The error impact rate has increased by 25 times. In the Brazilian disc splitting test, it is necessary to ensure the loading of the diameter as much as possible to prevent the error caused by the deviation loading.

From the above analysis, it can be seen that the maximum tensile stress should be at the intersection of the loading chord and the horizontal diameter when loading in chord direction. Substituting Equation (16) can obtain the modified theoretical equation of splitting tensile strength.

$$\sigma_t = \frac{P \cos \beta}{\pi t R}. \tag{22}$$

It can be seen from the above formula that as the β angle increases, the theoretical value of the tensile strength gradually decreases.

5. Conclusion

Aiming at the error of theoretical calculation caused by nonradial loading, this paper establishes the analytical expression of the stress of the disc under the chord loading by the theory of elastic mechanic complex function and analyzes the stress distribution law and the characteristic of splitting failure caused by the loading deviation. The main conclusions are as follows:

(1) Compared with radial loading, the disc exhibits a more intense stress concentration at the loading point under the bias loading, which tends to cause the disc to be crushed near the loading point without tensile damage. Under the deviation loading, except for the loading point areas on both sides, the tensile stress along the loading string is uniformly distributed, and the maximum tensile stress appears at the midpoint of the loading string; in addition, the tensile stress and compressive stress of the disk gradually increase along the horizontal diameter. The maximum value is reached at the intersection with the loaded string

(2) The maximum tensile stress and minimum compressive stress appear at the intersection of the loaded chord and the horizontal diameter. Therefore, it is easy to break the damage first under the chord loading. As the deviation angle increases, the tensile strength measured by the Brazilian split test decreases gradually, and the error impact rate gradually increases. Deviation loading will lead to a small test result. Under chord loading, the tensile strength should be calculated using the correction formula

(3) The proposed correction formula provides theoretical guidance for analyzing the nonradial cracking phenomenon of the disc. Additionally, more relevant experiments need to be done for understanding this issue in the next step

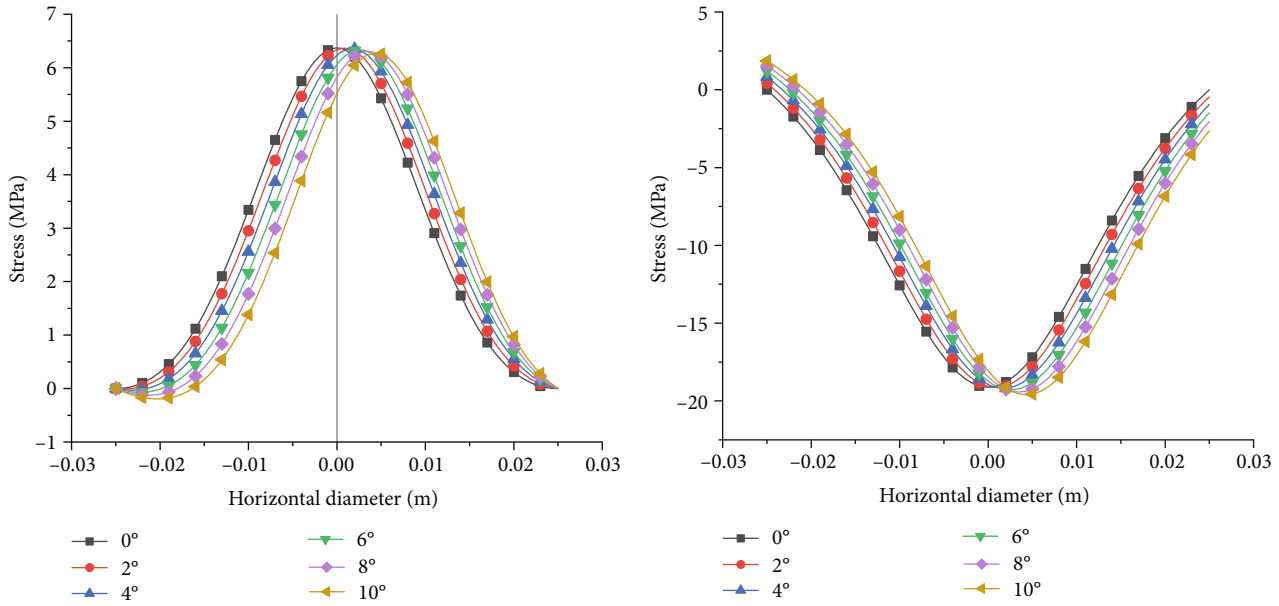

(a) Distribution of tensile stress

(b) Distribution of compressive stress

Figure 7: Stress distribution law along the horizontal diameter under different deviation angles.

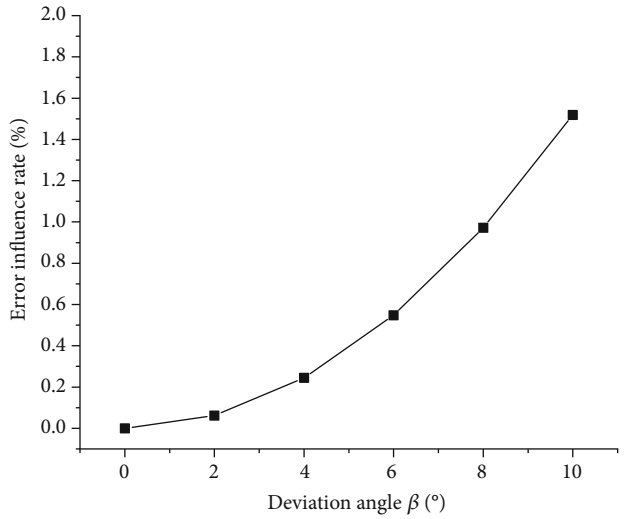

Figure 8: The evolution law of error impact rate with deviation angle.

Data Availability

The data used to support the findings of this study are included within the article.

Conflicts of Interest

The authors have no conflicts of interest.

Acknowledgments

This work is supported by the National Natural Science Foundation of China (51774196, 51774194, and 51578327), the National Natural Science Foundation of China and Shandong Province joint Program (U1806209), the China Postdoctoral Science Foundation (No. 2016M592221), the SDUST Research Fund (Grant/Award Number: 2019TDJH101), and the SDUST Young Teachers Teaching Talent Training Plan (BJRC20160501).

References

[1] Y. Tan, Q. Ma, Z. Zhao et al., "Cooperative bearing behaviors of roadside support and surrounding rocks along gob-side," *Geomechanics and Engineering*, vol. 18, no. 4, pp. 439–448, 2019.

[2] Z. Zhao, W. Sun, S. Chen, W. Wang, and Q. Wang, "Coupling model of jointed rock mass and rock bolt in offshore LPG underground storage," *Energy Science & Engineering*, pp. 1–16, 2019.

[3] Z. Zhao, Y. Tan, S. Chen, Q. Ma, and X. Gao, "Theoretical analyses of stress field in surrounding rocks of weakly consolidated tunnel in a high-humidity deep environment," *International Journal of Rock Mechanics and Mining Sciences*, vol. 122, article 104064, 2019.

[4] M. S. Diederichs and P. K. Kaiser, "Tensile strength and abutment relaxation as failure control mechanisms in underground excavations," *International Journal of Rock Mechanics and Mining Sciences*, vol. 36, no. 1, pp. 69–96, 1999.

[5] P. Hauseux, E. Roubin, D. M. Seyedi, and J. B. Colliat, "FE modelling with strong discontinuities for 3D tensile and shear fractures: application to underground excavation," *Computer Methods in Applied Mechanics and Engineering*, vol. 309, pp. 269–287, 2016.

[6] Z. Zhao, Q. Ma, Y. Tan, and X. Gao, "Load transfer mechanism and reinforcement effect of segmentally yieldable anchorage in weakly consolidated soft rock," *SIMULATION*, vol. 95, no. 1, pp. 83–96, 2019.

[7] M. A. Perras and M. S. Diederichs, "A review of the tensile strength of rock: concepts and testing," *Geotechnical and Geological Engineering*, vol. 32, no. 2, pp. 525–546, 2014.

[8] X. Z. Lyu, Z. H. Zhao, X. J. Wang, and W. M. Wang, "Study on the permeability of weakly cemented sandstones," *Geofluids*, vol. 2019, Article ID 8310128, 14 pages, 2019.

[9] C. C. Garcia-Fernandez, C. Gonzalez-Nicieza, M. I. Alvarez-Fernandez, and R. A. Gutierrez-Moizant, "Analytical and experimental study of failure onset during a Brazilian test," *International Journal of Rock Mechanics and Mining Sciences*, vol. 103, pp. 254–265, 2018.

[10] D. Li and L. N. Y. Wong, "The Brazilian disc test for rock mechanics applications: review and new insights," *Rock Mechanics and Rock Engineering*, vol. 46, no. 2, pp. 269–287, 2013.

[11] A. Basu, D. A. Mishra, and K. Roychowdhury, "Rock failure modes under uniaxial compression, Brazilian, and point load tests," *Bulletin of Engineering Geology and the Environment*, vol. 72, no. 3-4, pp. 457–475, 2013.

[12] C. Rocco, G. V. Guinea, J. Planas, and M. Elices, "Review of the splitting-test standards from a fracture mechanics point of view," *Cement and Concrete Research*, vol. 31, no. 1, pp. 73–82, 2001.

[13] ISRM Testing Commission, "Suggested methods for determining tensile strength of rock materials," *International Journal of Rock Mechanics and Mining Sciences & Geomechanics Abstracts*, vol. 15, no. 3, pp. 99–103, 1978.

[14] B. R. Indriyantho and Nuroji, "Finite element modeling of concrete fracture in tension with the Brazilian splitting test on the case of plane-stress and plane-strain," *Procedia Engineering*, vol. 95, pp. 252–259, 2014.

[15] D. Phueakphum, K. Fuenkajorn, and C. Walsri, "Effects of intermediate principal stress on tensile strength of rocks," *International Journal of Fracture*, vol. 181, no. 2, pp. 163–175, 2013.

[16] S. Y. Wang, S. W. Sloan, and C. A. Tang, "Three-dimensional numerical investigations of the failure mechanism of a rock disc with a central or eccentric hole," *Rock Mechanics and Rock Engineering*, vol. 47, no. 6, pp. 2117–2137, 2014.

[17] X. X. Wei and K. T. Chau, "Three dimensional analytical solution for finite circular cylinders subjected to indirect tensile test," *International Journal of Solids and Structures*, vol. 50, no. 14-15, pp. 2395–2406, 2013.

[18] C. F. Markides, D. N. Pazis, and S. K. Kourkoulis, "Closed full-field solutions for stresses and displacements in the Brazilian disk under distributed radial load," *International Journal of Rock Mechanics and Mining Sciences*, vol. 47, no. 2, pp. 227–237, 2010.

[19] Q. Z. Wang and L. Z. Wu, "The flattened Brazilian disc specimen used for determining elastic modulus, tensile strength and fracture toughness of brittle rocks: experimental results," *International Journal of Rock Mechanics and Mining Sciences*, vol. 41, no. 2, pp. 26–30, 2004.

[20] S. K. Kourkoulis, C. F. Markides, and P. E. Chatzistergos, "The standardized Brazilian disc test as a contact problem," *International Journal of Rock Mechanics and Mining Sciences*, vol. 57, pp. 132–141, 2013.

[21] C. F. Markides, D. N. Pazis, and S. K. Kourkoulis, "The Brazilian disc under non-uniform distribution of radial pressure and friction," *International Journal of Rock Mechanics and Mining Sciences*, vol. 50, pp. 47–55, 2012.

[22] M. Q. You and C. D. Su, "Theory and experiment of platform disc splitting," *Chinese Journal of Rock Mechanics and Engineering*, vol. 23, no. 1, pp. 170–174, 2004.

[23] J. Yu, X. Shang, and P. Wu, "Influence of pressure distribution and friction on determining mechanical properties in the Brazilian test: theory and experiment," *International Journal of Solids and Structures*, vol. 161, pp. 11–22, 2019.

[24] R. Yuan and B. Shen, "Numerical modelling of the contact condition of a Brazilian disk test and its influence on the tensile strength of rock," *International Journal of Rock Mechanics and Mining Sciences*, vol. 93, pp. 54–65, 2017.

[25] Y. Tong, W. Baoxue, S. Lin, and G. Qinghua, "Effects of various spacer methods for rock split tests," *Site Investigation Science and Technology*, vol. 1, pp. 3–7, 2002.

[26] K. Thuro, R. J. Plinninger, S. Zah, and S. Schutz, "Scale effects in rock strength properties. Part 1: unconfined compressive test and Brazilian test," in *ISRM Regional Symposium*, pp. 169–174, Espoo, Finland, June 2001.

[27] N. I. Muschelišvilli, *Some Basic Problems of the Mathematical Theory of Elasticity*, P. Noordhoff Ltd, 1953.